# Electric double-layer capacitor characteristics of activated wood charcoals

Ryohei Asakura*, **❖, Tetsuo Kondo**, Mitsuhiro Morita**, Hiroaki Hatori*** and Yoshio Yamada****

The electric double-layer　EDL　capacitor characteristics of five types of wood charcoals were compared with those of two commercially available activated carbon fibers　ACFs　. Although the specific surface areas of the charcoals were lower than those of the ACFs, the charcoals gave EDL capacitance values comparable to those of the ACFs. Nitrogen adsorption isotherms revealed that the pore structure of the wood charcoals was composed of both micropores and mesopores, whereas the ACFs consisted mainly of micropores. This finding suggests that mesopores in the charcoals play an important role in the formation of the EDL. The cyclic charge-discharge behavior, which is closely related to the permeation or diffusion of the electrolyte ions into the pores, indicated that the rate of permeation of the electrolyte in the wood charcoals was faster than that in the ACFs. The degree of EDL capacitance and the cyclic charge-discharge behavior reflect the difference in pore structure between the wood charcoals and the ACFs.

## 1　Introduction

The electric double-layer　EDL　capacitor is an energy storage device based on the phenomenon that an EDL is formed at the boundary between an electrode surface and an electrolyte[1]. EDL capacitors composed of a pair of porous carbon materials such as activated carbons are expected to be applicable as startup devices for fuel cell and hybrid cars[2 -4]. Activated carbons are used for EDL electrodes because their large specific surface areas are suitable for both adsorption and desorption of electrolyte ions without electrochemical reactions and because they are highly electrically conductive, enabling rapid and complete charge-discharge cycles. Thus, in recent years various types of activated carbons have been synthesized in an attempt to develop high-power EDL capacitors[5 -8].

Carbonization of wood into charcoal is an effective end-use of wood. Wood charcoal has traditionally been used as a fuel, as an adsorbent, and for soil improvement and humidity control. A potential new application for wood charcoal involves transformation of the charcoal to suitable porous activated carbons for use in EDL capacitors.

Wood is a naturally occurring composite material composed of cellulose, hemicellulose, lignin, extractives, and inorganic compounds distributed heterogeneously in a cell wall structure[9]. Wood has been used as a raw material for activated carbons, but there are important differences between wood and other raw materials such as coals, tar pitch, and synthetic resins. For example, oxygen is much more abundant in wood than in coals and tar pitch, and, unlike synthetic resins, wood has difficulty in controlling three-dimensional structure artificially. In addition, the presence of impurities, inhomogeneity, and low yield are problematic in manufacturing activated carbon from wood. However, if the unique structural features of wood could be maintained during carbonization and activation processes, activated carbons with well-defined pore sizes could be obtained. It is well-known that pore structure plays an important role in EDL formation. However, there have been few studies on the use of wood charcoal for electrodes of EDL capacitors[10].

In the present study, we compare the capacitor characteristics of wood charcoals with those of commercial activated carbon fibers　ACFs　. On the basis of EDL capacitor performance and pore structure, which affects performance, we discuss the possibility of preparing EDL capacitor electrodes from wood charcoal.

## 2　Experimental

### 2.1　Sample preparation

Three types of hardwood charcoals　lauan　AC-La　, Japanese

❖　Corresponding Author, E-mail: rasakura@fitc.pref.fukuoka.jp
*　Fukuoka Industrial Technology Center, Interior Design Research Institute　405-3 Agemaki, Okawa, Fukuoka 831-0031, Japan
**　Biomacromolecular Materials Laboratory, Department of Forest and Forest Products, Graduate School of Agriculture, Kyushu University　6-10-1 Hakozaki, Higashi-ku, Fukuoka 812-8581, Japan
***　National Institute of Advanced Industrial Science and Technology　16-1 Onogawa, Tsukuba, Ibaraki 305-8569, Japan
****　Department of Materials Science　Engineering, Faculty of Engineering, Fukui University　3-9-1 Bunkyo, Fukui 910-8507, Japan

red oak (AC-Akg), and mangrove (AC-Man) and two types of softwood charcoals Japanese red pine (AC-Aka) and larch (AC-Kara) were used. The samples were powders with a particle size below 42~80 mesh. Each sample (7~12 g) was heated to 1173 K at a heating rate of 5 K/min under a nitrogen flow of 200 cm³/min, kept at this temperature for 1 h, and then cooled to room temperature. The carbonized samples (0.8~1.4 g) were activated at 1153 K for 15 min by a carbon dioxide flow of 200 cm³/min and then treated in the same way as explained above. Though capacitor performance is influenced by factors such as specific surface area, pore size distribution, surface functional groups, and impurities in the electrode material, the specific surface area of the electrode material can be regard as the most important factor. Therefore two types ACFs with different specific surface areas (ACF 1 and ACF 2) prepared from commercially available pitch-based carbon fibers were used as references.

## 2.2 Capacitance measurement

A conventional three-electrode cell was used to measure the capacitance. The composite disc electrode (diameter 13 mm) was prepared from ground carbon (ca. 40 mg), acetylene black (conductive material 5 mg), and poly (tetrafluoroethylene) powder (binder 5 mg) in an 8:1:1 weight ratio. A titanium mesh (40 mesh) was selected as a current collector for the disc electrode, and an identical mesh was used for the counter electrode. The charge-discharge cycles were carried out under galvanostatic conditions (2 mA, 0.2 to −0.7 V vs. Ag/AgCl, potential sweep range 0.9 V) in 1.0 M sulfuric acid electrolyte. For convenience, positive potential change was defined as "charge", and negative potential change as "discharge". The capacitance data were calculated from the discharge curve by using the following equation (Fig.1)

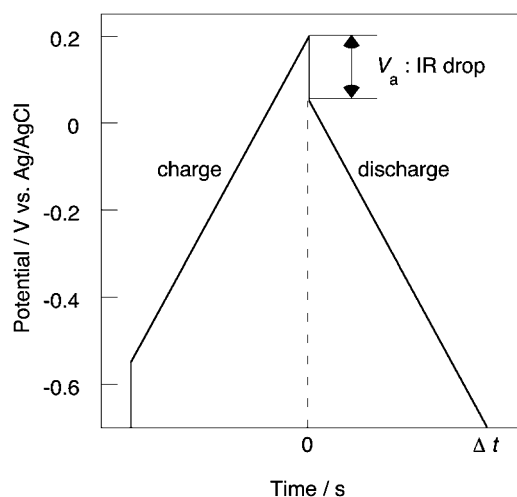$$\text{Capacitance[F/g]} = i \times \frac{\Delta t}{(0.9 - V_a) \times W} \quad \cdots\cdots (1)$$



**Fig.1** Potential-time curve at constant current.

where $i$ is the discharge current, $\Delta t$ is the discharge time, $V_a$ is the IR (current $I$ times resistance $R$) drop, and $W$ is the weight of the carbon. At equilibrium (i.e., when electrolyte ions cease to permeate the electrode), the continuous increase or decrease in the change in the discharge time during the last five charge-discharge cycles was not observed, and no further capacitance measurements were made.

## 2.3 Pore characteristics

Information on the pore structure of the carbon products was obtained from nitrogen adsorption isotherms at 77 K. The isotherms were measured with a BELSORP 18 PLUS (BEL Japan Co. Ltd., Osaka, Japan) instrument. The specific surface area was estimated from BET analysis[11], and the micropore volume and external specific surface area were evaluated by the subtracting pore effect (SPE) method[12, 13] using $\alpha_s$ plots. Total pore volume was calculated from the amount of nitrogen adsorbed by extrapolation to $P/P_0 = 1$. Average pore diameters were calculated on the assumption that the pores had a slit-type structure.

## 3 Results and Discussion

### 3.1 Elemental analysis, carbonization yield, and burn-off (Table 1)

Elemental analysis revealed that the wood charcoals and ACFs contained 82.1~93.1% and 85.1~89.1% carbon, respectively. The amounts of oxygen, hydrogen, and nitrogen in the samples did not vary much between samples. However, the ash content of the wood charcoals varied considerably from sample to sample.

The carbonization yield of the wood charcoals was around 20% regardless of the sample species. However, burn-off by activation varied from 15.3% to 33.7% (no data were obtained for AC-Akg) even under the same conditions. It is not clear why the burn-off values were different for the various woods, but the reactivity of the carbonized charcoals to CO₂ may influence the degree of burn-off as well as the formation of pores on activation.

**Table 1** Elemental analysis, carbonization yield, and burn-off by activation.

| sample | elemental analysis[a] | | | | | yield[c] | burn-off[d] |
|---|---|---|---|---|---|---|---|
| | C | H | O[b] | N | ash | | |
| AC-La | 82.1 | 1.2 | 12.9 | 0.2 | 3.7 | 22.0 | 33.7 |
| AC-Akg | 85.9 | 1.3 | 10.5 | 0.2 | 2.1 | 19.8 | N.D.[e] |
| AC-Man | 87.5 | 0.9 | 9.5 | 0.2 | 2.0 | 20.0 | 33.7 |
| AC-Aka | 91.0 | 0.8 | 7.3 | 0.1 | 0.8 | 20.4 | 22.1 |
| AC-Kara | 93.1 | 0.6 | 5.5 | 0.1 | 0.7 | 21.6 | 15.3 |
| ACF 1 | 85.4 | 1.4 | 12.7 | 0.6 | 0.0 | | |
| ACF 2 | 89.8 | 0.9 | 9.0 | 0.3 | 0.0 | | |

a   samples after activation.
b   the oxygen content was determined by difference.
c   weight after carbonization / weight of raw material × 100.
d   weight loss after activation / weight before activation × 100.
e   no data.

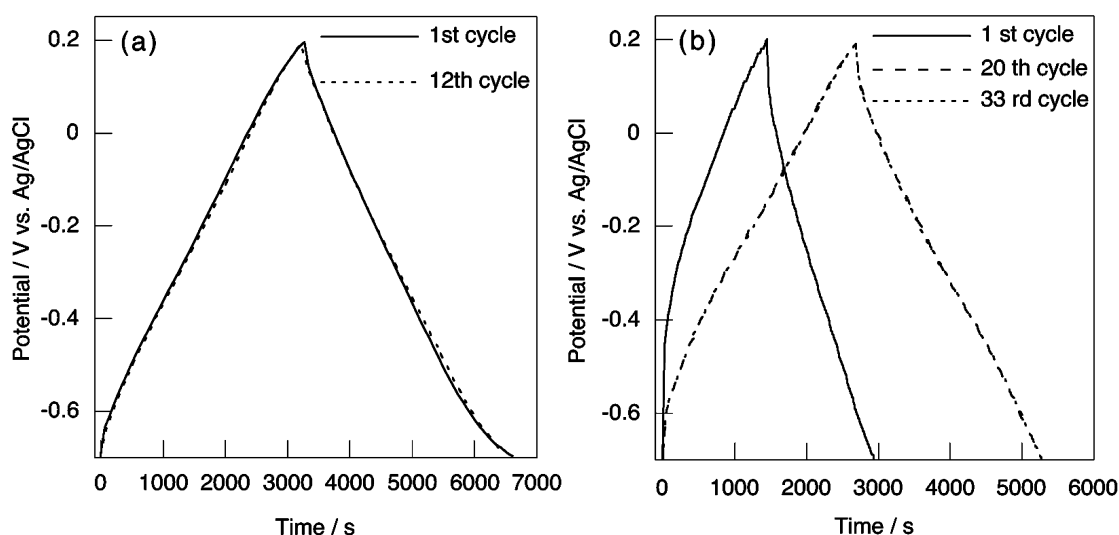**Fig.2** Potential-time curves for （a）AC-La and （b）ACF 1.

## 3.2 Variation of charge-discharge curve with cycle number

The charge-discharge curves of the first and final cycles for AC-La （**Fig.2**a） and ACF 1 （**Fig.2**b） showed that the samples performed differently with increasing cycle number. The curves for AC-La are almost the same between the 1st and 12th cycles, except for a small decrease in the charge-discharge time. In contrast, the charge-discharge time for ACF 1 became gradually longer with increasing cycle number from the 1st to the 16th cycle； thereafter it remained constant until the 33rd cycle. The curves for the 1st, 20th, and 33rd cycles are shown in **Fig.2**b. The difference in the cycling curves for AC-La and ACF 1 can be explained in terms of the permeability of the electrode to electrolyte ions； that is, the difference in the cycling curves suggests that the electrolyte ions in solution can diffuse more easily into the AC-La electrode than into the ACF 1 electrode. For electrodes prepared from wood charcoals, the charge-discharge time changed only slightly over several tens of cycles. The ACF 2 electrode showed the same tendency as the ACF 1 electrode.

## 3.3 Capacitance with charge-discharge cycles

The variation of the EDL capacitance with cycle number is shown in **Fig.3**. Each capacitance value was obtained from the discharge curve measured at a constant current of 2 mA. The capacitance for ACF 1 and ACF 2 increased rapidly with increasing cycle number, whereas that for the wood charcoals was almost constant.

## 3.4 Nitrogen adsorption isotherms

The pore structure of the carbon material used for the electrode influences the performance of EDL capacitors. To clarify the relationship, we examined the nitrogen adsorption isotherms for the activated wood charcoals from hardwood （**Fig.4**a）, softwood （**Fig.4**b）, and ACFs （**Fig.4**c）.

The shapes of the adsorption isotherms of the five wood charcoals （**Figs.4**a, **4**b） are similar, though the amount of nitro-
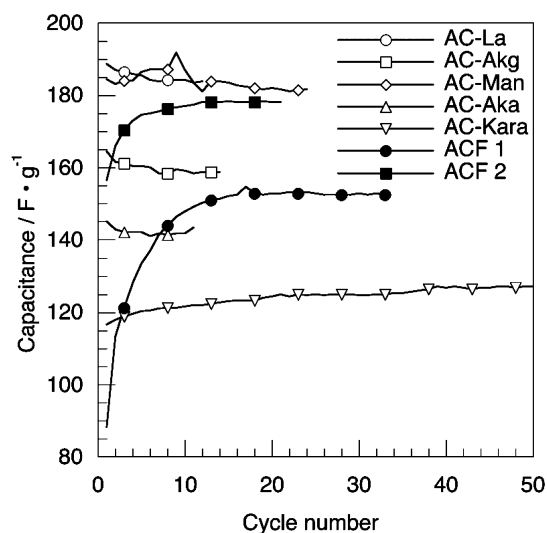


**Fig.3** Relationship between number of discharge cycles and capacitance.

gen adsorbed varies among the charcoals. These isotherms show a steep rise in nitrogen adsorption at low relative pressure followed by a gradual increase at higher relative pressure. In addition, hysteresis loops are observed. According to the adsorption isotherm classification of IUPAC[14], these adsorption isotherms are composed of type I （microporous） and type III （mesoporous） isotherms. Furthermore, the hysteresis loops are almost type H4 hysteresis loops. Thus, **Figs.4**a, **4**b indicate that the charcoals contain a considerable amount of micropores as well as mesopores and that the mesopores have a slit-like shape. In contrast, the ACF isotherms show a steep rise in nitrogen adsorption at low relative pressure followed by saturation at higher pressure, and no hysteresis loops are observed （**Fig.4**c）. The ACF isotherms are classified as typical type I isotherms containing mainly micropores.

## 3.5 Relationship between capacitance and pore structure

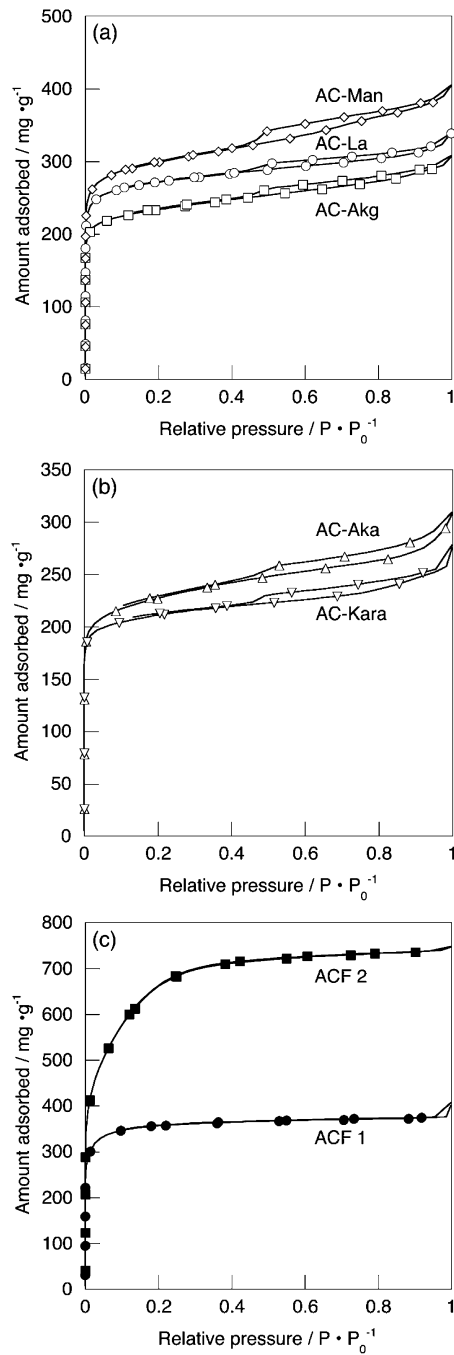EDL capacitance and pore characteristics are summarized in

**Fig.4** Nitrogen adsorption isotherms for (a) hardwoods, (b) softwoods, and (c) ACFs.

**Table 2**. The EDL capacitance (Capacitance) values shown in **Fig.3** are those at the last cycle (127–184 F/g) for the wood charcoals, and 153 and 178 F/g for ACF 1 and ACF 2, respectively. The capacitance values of the AC-La, AC-Akg, and AC-Man samples are comparable to those of the ACF samples. On the basis of $\alpha_s$ plots, all samples are F-type samples except ACF 2, which is an FC-type sample. According to the SPE method, the total specific surface area of an F-type sample cannot be estimated from an $\alpha_s$ plot. Consequently, in this study, we used the specific surface areas obtained from BET analyses. The specific surface areas $a_{BET}$ for the wood charcoals range from 659 to 924 m²/g, whereas the $a_{BET}$ values for ACF 1 and ACF 2 are 1123 and 1744 m²/g, respectively. Even the specific surface area of AC-Man, which has the largest specific surface area of the five wood charcoals, is smaller than that of ACF 1. It is interesting that, in spite of their relatively small specific surface areas, AC-La, AC-Akg, and AC-Man have capacitance values roughly comparable to those of ACF 1 and ACF 2.

To assess the number of pores contributing to formation of the electric double layer, we calculated the EDL capacitance per unit specific surface area (Capacitance$_{BET}$ (Capacitance/$a_{BET}$)). The Capacitance$_{BET}$ of the wood charcoals was around 0.200 F/m², whereas the Capacitance$_{BET}$ of the ACFs was only 0.136 and 0.102 F/m². This result indicates that fewer pores contribute to formation of the electric double layer in the ACFs than in the wood charcoals. To discuss this point in detail, we obtained the following (average micropore diameter, average mesopore diameter, and total pore diameter, assuming slit-type pores) the ratio $a_{ext}/a_{BET}$ ($a_{ext}$ is the external specific surface area, excluding micropores) and micropore volume as a fraction of total pore volume. Comparison of $a_{ext}/a_{BET}$ and $V_{micro}/V_{total}$ showed that micropores occupied a greater portion of the total pore volume in the ACFs than in the wood charcoals. The value of $w_{avg}$ was around 1 nm except for ACF 1, $w_{micro}$ was around 0.8 nm except for ACF 2, and $w_{meso}$ varied from 2.00 to 3.10 nm. The ACFs are mainly composed of micropores, whereas the wood charcoals have a wide distribution of micropores and mesopores. Endo *et al.*[15] reported the relationship

**Table 2** EDL capacitance and pore characteristics

| sample | Capacitance[a] F/g | $a_{BET}$[b] m²/g | Capacitance$_{BET}$[c] F/m² | $a_{ext}$[d] m²/g | $a_{ext}/a_{BET}$[e] | $V_{micro}$[d] cm³/g | $V_{total}$[f] cm³/g | $V_{micro}/V_{total}$[g] | $w_{avg}$[h] nm | $w_{micro}$[i] nm | $w_{meso}$[j] nm |
|---|---|---|---|---|---|---|---|---|---|---|---|
| AC-La | 184 | 841 | 0.219 | 77 | 9.2 | 0.304 | 0.410 | 72.6 | 1.00 | 0.80 | 2.98 |
| AC-Akg | 159 | 721 | 0.220 | 92 | 12.8 | 0.251 | 0.368 | 68.2 | 1.02 | 0.80 | 2.50 |
| AC-Man | 182 | 924 | 0.197 | 165 | 17.9 | 0.292 | 0.491 | 59.5 | 1.06 | 0.77 | 2.41 |
| AC-Aka | 143 | 693 | 0.207 | 78 | 11.3 | 0.254 | 0.375 | 67.7 | 1.08 | 0.79 | 3.10 |
| AC-Kara | 127 | 659 | 0.193 | 55 | 8.3 | 0.238 | 0.322 | 73.9 | 0.98 | 0.83 | 3.05 |
| ACF 1 | 153 | 1123 | 0.136 | 28 | 2.5 | 0.435 | 0.466 | 93.3 | 0.83 | 0.79 | 2.21 |
| ACF 2 | 178 | 1744 | 0.102 | 80 | 4.6 | 0.835 | 0.915 | 91.3 | 1.05 | 1.00 | 2.00 |

a Dischrge current 2 mA. b estimated from $P/P_0$ at 0.01–0.05. c Capacitance/$a_{BET}$. d SPE method. e $a_{ext}/a_{BET} \times 100$.
f $P/P_0$ extraplorated to 1. g $V_{micro}/V_{total} \times 100$. h assuming slit-like pores. $2V_{total}/a_{BET}$. i assuming slit-like pores. $2V_{micro}/(a_{BET} - a_{ext})$.
j assuming slit-like pores. $2(V_{total} - V_{micro})/a_{ext}$.

between electrolyte and pore size of activated carbons. In their paper, Endo *et al*. used the literature value for the average diameter of sulfate anion, 0.533 nm. The difference in Capacitance$_{BET}$ values between the wood charcoals and the ACF samples can be explained in terms of the size of the sulfate anion and the pore diameters of the carbons. The ACF samples mainly have pores with diameters corresponding to only 1 or 2 sulfate anion diameters, allowing only 1 or 2 sulfate anions to reach the pore surface. In contrast, in addition to the small ACF-type pores, the wood charcoals have much larger pores, allowing multiple sulfate anions to reach the pore surface. Moreover, the ratio of micropores to mesopores might influence the capacitance. Therefore, a suitable combination of micropores and mesopores in the activated charcoal may be effective for diffusion of ions into the porous electrode. However, it is necessary and important to clarify that the wood charcoals employed in this study, and wood charcoals in general, have both mesopores and micropores.

## 4　Conclusion

The EDL capacitor characteristics of electrodes prepared from five types of wood charcoals and two commercial ACFs were investigated in connection with their pore structures. Three of the five types of wood charcoals showed capacitance comparable to that of the ACFs, although the former carbons had lower specific surface areas than the latter. Pore structure influenced EDL capacitor performance. The wood charcoals were composed of both micropores and mesopores, whereas the ACFs consisted mainly of micropores. Diffusion of electrolyte through the wood charcoals was faster than through the ACFs because the wood charcoals consisted of both small micropores and larger mesopores, whereas the ACFs consisted mainly of small micropores. The specific surface areas of the wood charcoals varied from sample to sample, even though the five types of wood charcoals were prepared under the same activation conditions. The reason for this variation of specific

surface area and the nature of the mesopore/micropore structure need to be clarified to develop new applications for wood charcoal. Wood charcoal may be a suitable material for EDL capacitors.

## References

1　B. E. Conway, "Electrochemical Supercapacitors　Scientific Fundamentals and Technological Applications"　Kluwer Academic/ Plenum Publishers, New York, 1999　p.105.

2　B. E. Conway, "Electrochemical Supercapacitors　Scientific Fundamentals and Technological Applications"　Kluwer Academic/ Plenum Publishers, New York, 1999　p.663.

3　A. Nishino, *J. Power Sources* **60**　1996　137-147.

4　M. Okamura, H. Hasuike, M. Yamagishi and S. Araki, *Electrochemistry* **69**　6　2001　414-421.

5　Y. Sakata, A. Muto, M. A. Uddin, N. Yamada, C. Marumo, S. Ibaraki and K. Kojima, *Electrochemical and Solid-State Letters* **3**　1　2000　1-3.

6　H. Nakagawa, A. Shudo and K. Miura, *J. Electrochem. Soc*. **147**　1　2000　38-42.

7　Y. Yamada, O. Tanaike, T. Liang, H. Hatori, S. Shiraishi and A. Oya, *Electrochemical and Solid-State Letters* **5**　12　2002　A283-285.

8　S. Shiraishi, H. Kurihara and A. Oya, *Electrochemistry* **69**　6　2001　440-443.

9　D. Fengel and G. Wegener, "Wood. Chemistry, Ultrastructure, Reactions"　Walter de Gruyter. Berlin　New York, 1984　pp.227-239.

10　N. Yamada, A. Muto, M. A. Uddin, K. Kojima, S. Ibaraki, C. Marumo and Y. Sakata, *Electrochemistry* **69**　6　2001　434-436.

11　F. Rouquerol, J. Rouquerol and K. S. W. Sing, "Adsorption by Powders & Porous Solids"　Academic Press, New York, 1999　p.165.

12　K. Kaneko and C. Ishii, *Colloids Surf*. **67**　1992　203-212.

13　K. Kaneko, C. Ishii, M. Ruike and H. Kuwabara, *Carbon* **30**　7　1992　1075-1088.

14　K. S. W. Sing, *Pure Appl. Chem*. **57**　1985　603-619.

15　M. Endo, T. Maeda, T. Takeda, Y. J. Kim, K. Koshiba, H. Hara and M. S. Dresselhaus, *J. Electrochem. Soc*. **148**　8　2001　A910-A914.